Space Weather

RESEARCH ARTICLE
10.1029/2023SW003743

Characterization of the Ionospheric Vertical Error Correlation Lengths Based on Global Ionosonde Observations

L. Yuan[1], **Timothy Kodikara**[1], **and M. M. Hoque**[1]

[1]Institute for Solar-Terrestrial Physics, German Aerospace Center (DLR), Neustrelitz, Germany

Key Points:

- Derives ionospheric vertical correlation lengths (VCLs) from global ionosondes
- Demonstrates that the variance ratio between model and measurements can characterize the ionospheric error VCL
- Proposes a novel ionospheric VCL model based on modeling the variance ratio and vertical scale heights

Correspondence to:

L. Yuan,
liangliangyuan1994@gmail.com

Citation:

Yuan, L., Kodikara, T., & Hoque, M. M. (2024). Characterization of the ionospheric vertical error correlation lengths based on global ionosonde observations. *Space Weather*, *22*, e2023SW003743. https://doi.org/10.1029/2023SW003743

Received 28 SEP 2023
Accepted 19 FEB 2024

Author Contributions:

Conceptualization: L. Yuan
Data curation: L. Yuan
Formal analysis: L. Yuan
Funding acquisition: M. M. Hoque
Investigation: L. Yuan
Methodology: L. Yuan
Project administration: M. M. Hoque
Resources: L. Yuan
Software: L. Yuan
Validation: L. Yuan
Writing – original draft: L. Yuan
Writing – review & editing: L. Yuan, Timothy Kodikara, M. M. Hoque

Abstract Data assimilation is one of the most important approaches to monitoring the variations of ionospheric electron densities. The construction of the background error covariance matrix is an important component of ionospheric data assimilations. To construct the background error covariance matrix, the information about the spatial ionospheric correlations is required. We present a statistical analysis on the ionospheric vertical error correlation length (VCL) based on a global network of ionosondes and the Neustrelitz Electron Density Model. We show that the locally derived VCL is well-defined and the VCL does not show a considerable dependency on the geographical seasons while local time dependencies of the VCL are shown to be present. A novel VCL model is also established based on the ionospheric scale heights. We show that the ionospheric VCL can be characterized by the variance ratio between the ionosphere model and ionospheric measurements. The altitudinal variations of VCLs are controlled by the interactions between the inherent VCLs of the ionosphere model and the measurements. Two experiments are conducted at two different latitudes based on the proposed model. The results show that the proposed model is stable and well-correlated with the observed VCLs, which implies a potential to be generalized for a global correlation model. The proposed model can be used in the temporal evolution of error covariance matrices in the ionospheric 4D-Variational (4D-Var) assimilations, which may overcome the main drawbacks of the static error covariance specifications in the ionospheric 4D-Var assimilations.

Plain Language Summary In ionospheric data assimilations, one of the most important pieces of information is the background error correlation, which controls the spatial spread of observations. In this study, the vertical error correlation length (VCL) will be evaluated locally based on a statistical analysis using the Neustrelitz Electron Density Model and global ionosonde observation network from Global Ionospheric Radio Observatory. For the first time, this study establishes that ionospheric VCLs can be effectively characterized by two primary parameters: the variance ratio and the correlation between the ionospheric model and the observational data. In addition, the study examines the relationships between climatological VCLs and scale heights within empirical ionospheric models. A novel VCL model is proposed based on the statistical analyses. The proposed correlation length models offer utility in the temporal evolution of error covariance matrices within ionospheric 4D variational assimilations, potentially mitigating one of the primary limitations associated with static error covariance specifications in such assimilation procedures.

1. Introduction

Data assimilation is one of the most important approaches to monitoring the variations of ionospheric electron densities. During the past two decades, several assimilation tools were developed, such as the Ionospheric Data Assimilation Four-Dimensional (IDA4D), Global Assimilative Ionospheric Model (GAIM (Bust & Crowley, 2007; Bust & Datta-Barua, 2014; Bust & Mitchell, 2008; Bust et al., 2004) and Neustrelitz Electron Density Assimilative Model (NEDAM) (Yuan et al., 2023). Although the detailed strategies among all assimilation tools may differ, one of the main challenges of data assimilations is the lack of knowledge about the error covariance information of the background model. The correlations among ionospheric electron densities are not only important for a better understanding of the ionospheric physical processes which determine the behavior of ionosphere but also an essential part in the data assimilations (Daley, 1991; Scherliess et al., 2006; Shim et al., 2008; Yuan et al., 2023).

The construction of the background error covariance matrix is an important component of ionospheric data assimilation algorithms. For data assimilations with physics-based background models, it is often beneficial to

estimate the background error covariances via the ensemble method (Codrescu et al., 2018; Kodikara et al., 2021; Yue, Wan, Liu, & Mao, 2007; Yue, Wan, Liu, Zheng, et al., 2007). To construct the background covariance matrix, the information about the spatial ionospheric correlations is required. It is commonly assumed that the horizontal and vertical components are independent (Bust et al., 2004; Yue et al., 2011; Yue, Wan, Liu, & Mao, 2007; Yue, Wan, Liu, Zheng, et al., 2007). The horizontal correlation matrix describes the correlations between all the grid points and determines the area influenced by observations. Shim et al. (2008) have used more than 150 million total electron density (TEC) observations from more than 1,000 globally distributed Global Positioning Satellite (GPS) system ground receivers to study the local and spatial morphology of day-to-day ionospheric variability. Forsythe et al. (2020) estimate the horizontal correlation lengths using 20 years of GPS total electron content (TEC) values from the Jet Propulsion Laboratory Global Ionospheric Maps (GIMs) for different seasons, geomagnetic conditions, and universal times. It was found that the global distributions of the zonal and meridional correlation lengths between the two approaches are very different and that the correlation lengths derived from day-to-day TEC variability cannot be used as a proxy for the construction of a covariance matrix for ionospheric data assimilation.

However, there are only few studies on the ionospheric vertical correlations. The vertical error correlation matrix as well as the background model itself determine the form of the assimilated electron density profile. It is shown that the vertical part of the covariance model plays the most important role because it preserves the vertical structure of the F-region density layer and helps to correct a tomographic issue that arises when the slant total electron content is assimilated along the intersecting rays (Forsythe, Azeem, Blay, et al., 2021). But at the same time, large correlations especially in the peak density regions prevent the change of peak density heights. It is also suggested that the intersected observations need to be weighted properly by introducing the non-zero off-diagonal terms in the observation covariance matrice (Yuan et al., 2023). Forsythe, Azeem, Crowley, and Themens (2021) evaluated the vertical error correlation length (VCL) of electron densities based on a statistical analysis using IRI2016 and 5 operational incoherent scatter radar (ISR) stations. However, the spatial limitation of the statistical analysis is inevitable since the ISR stations are sparsely located and restricted within a narrow longitudinal sector. Moreover, the VCL defined in Forsythe, Azeem, Crowley, and Themens (2021) is the distance where the correlation coefficient is equal to 0.7. It is worth noting that the VCL defined there indeed represents an "average" VCL between the reference height and the height where the linear correlation coefficient is equal to 0.7. And they proposed an asymmetric (or anisotropic) strategy for modeling the VCL, which leads to an asymmetric covariance matrix rather than a symmetric covariance matrix. Instead of using some simple empirical reference values for the vertical error VCLs, it is more beneficial to derive a more realistic model for VCLs based on statistical analyses using real observations.

In this study, the VCL will be evaluated locally based on a statistical analysis using the Neustrelitz Electron Density Model (NEDM) and global ionosonde observation network from Global Ionospheric Radio Observatory (GIRO). In Section 2, we describe the ionosphere model and data set as well as the processing strategies for our statistical analyses. The proposed methods are presented in Section 3. The main results of ionospheric VCLs are demonstrated and discussed in Section 4. A statistical characterization of VCLs is realized by relating the VCLs with ionospheric scale heights. We develop a novel VCL model based on the above mentioned characterizations. In order to validate the VCL models, two experimental analyses were also performed at the GA762 and LV12P ionosonde stations. Finally, major conclusions and future tasks are given in Section 5.

2. Ionosphere Model and Data Processing

2.1. Neustrelitz Electron Density Model

The ionospheric plasma density shows both the long-term (climatology) and short-term (weather) variations. The electron density distribution of the Earth's ionosphere can be modeled by adding a Chapman layer (Rishbeth & Garriott, 1969), representing the ionospheric F-layer N_{eF} with an E-layer N_{eE} model superposed by exponential decay functions representing the plasmasphere N_{eP}.

$$N_e = N_{eE} + N_{eF} + N_{eP}$$

This model describes the spatial and temporal variability of the above-mentioned key parameters as a function of local time, geographic or geomagnetic location, solar irradiation, and solar activity. Hoque et al. (2022) present a

comprehensive validation of NEDM using in-situ data from DMSP (Defense Meteorological Satellite Program), Swarm, Van Allen Probes and ICON (Ionospheric Connection Explorer) missions, topside TEC data from the COSMIC/FORMOSAT-3 mission, bottom-side TEC data from the TOPEX/Poseidon mission, and ground-based TEC data from the International GNSS Service (IGS) covering both high and low solar activity conditions. The NEDM has heritage in a family of ionospheric models developed at the German Aerospace Center (DLR) in Neustrelitz over the last 20 years. These include global empirical models for the ionospheric TEC, F2-layer peak density NmF2, and peak density height hmF2, which are used in operational space weather services. The NEDM is composed of the following domain-specific models. In the Neustrelitz Peak Density Model (Hoque & Jakowski, 2011), the basic modeling approach includes five major dependencies of Nm on the local time, season, geomagnetic latitude, equatorial anomaly, and solar cycle, and they are combined in a multiplicative way as

$$N_m = \prod_{i=1}^{5} F_i$$

The factor F_i explicitly contains the model functions and coefficients (Hoque & Jakowski, 2011). In the Neustrelitz Peak Height Model (Hoque & Jakowski, 2012), following the same basic approach as N_m, a set of nonlinear equations describing the dependencies of h_m on local time, season, geomagnetic field, and solar activity are combined in a multiplicative way (for details, see Hoque & Jakowski, 2012). The local time variation contains the diurnal, semidiurnal, and terdiurnal harmonic components as well as dependency on the solar zenith angle. In the Neustrelitz TEC Model (NTCM) the major dependencies of TEC are combined in a multiplicative way, similar to the Nm model (Jakowski et al., 2011). The factors explicitly contain the model functions and coefficients whose number varies between 2 and 6 for different factors. A background ionosphere electron density model is essential in data assimilations to provide apriori information and fill in areas where there are no available data. The accuracy of the background model in a climatological sense is one of the most important factors that affect the success of data assimilation, since the background covariance information is highly dependent on the background model. In order to achieve complete coverage from ground to GPS satellites, the background ionosphere model will also need to include a plasmasphere model, since plasmaspheric electron content may contribute more than 60% of the total TEC in the line-of-sight direction, especially during the local night. And recently Jakowski and Hoque (2018) developed an empirical Neustrelitz Plasmasphere Model (NPSM) based on electron density data derived from topside GPS measurements onboard the Challenging Minisatellite Payload (CHAMP) satellite. The NPSM describes electron density distribution in the topside ionosphere and plasmasphere by addressing not only McIlwain L-shell dependencies of the electron but also by considering the coupling with the ionosphere and altitude dependencies. Although the number of model coefficients and parameters is rather small, these four models describe the main ionospheric/plasmaspheric features with good quality. Each sub-model is driven by the solar radio flux index F10.7 and the 3D global outputs are realized by combining multiple Chapman layers with a superposed exponential decay function describing the plasmasphere. Apart from NEDM, a new assmilative model NEDAM was recently developed based on a 4D-Variational (4D-Var) approach by Yuan et al. (2023). The background electron density model NEDM may contain the climatological variation of the ionosphere while the assimilation NEDAM refines the background model with the short-term variations.

2.2. Global Ionosonde Observations

The Global Ionosphere Radio Observatory (GIRO) provides a global network of ionosondes with a considerably high reliability and continuity. Figure 1 shows the geographical distributions of ionosonde stations used in this study from the GIRO network in the solar maximum year (2013) and solar minimum year (2018). The blue dots represent the available ionosondes in both years while the red dots represent the available ionosondes in 2018. Ionograms are recorded tracings of reflected high-frequency radio pulses generated by an ionosonde. Unique relationships exist between the sounding frequency and the ionosphere plasma densities which can reflect the radio signal. In order to make the electron density profile uniformly organized, the electron density profiles are interpolated with a step size of 5 km. It is worth mentioning that the ionosonde-derived electron density profiles are valid below the peak density height and artificial above the peak density height due to the Chapman-extrapolation. During nighttime, the detectable ranges of the ionosonde might be lower, since the solar radiation is absent. The whole data set is divided into two subsets according to the local time, that is, day (09–15hr LT) and night (21–03hr LT). Due to the possible discontinuity of the ionosonde data, it is crucial to remove the

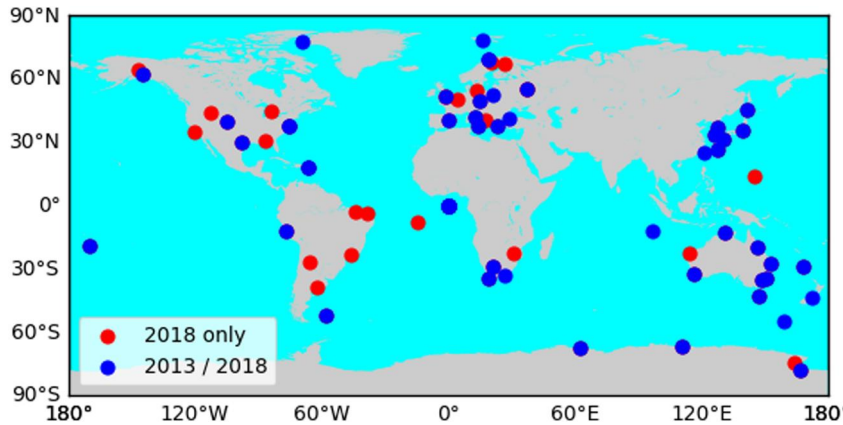

Figure 1. Geographical distribution of ionosonde stations from the GIRO network used in this study in the solar maximum year 2013 and the solar minimum year 2018. The red dots represent the available ionosonde stations in 2018 only, and the blue dots represent the available ionosonde stations in both 2013 and 2018.

discontinuity data points from the whole data set. A standard deviation filter is implemented for filtering ionosonde data, which means that the ionosonde from two standard deviations are removed.

3. Methods

3.1. The Vertical Correlation Length in NEDAM

In NEDAM, the 4D-Var problem is formulated as

$$J(x(t_0)) = \frac{1}{2}\left[\left(x(t_0) - x_o^b(t_0)\right)^T B_0^{-1}\left(x(t_0) - x_o^b(t_0)\right) + \sum_k \left(y_k - Hx(t_k)\right)^T R_k^{-1}\left(y_k - Hx(t_k)\right)\right] \quad (1)$$

where $x(t_0)$ represents the analysis state variable at time t_0, $x_o^b(t_0)$ the background state variable at time t_0, B_0^{-1} the background precision matrix, y_k the observation at time t_k, H the design matrix, R_k^{-1} the observation precision matrix and $x(t_k)$ the predicted state variable at time t_k. The state variable $x(t_0)$ to be analyzed could be estimated based on a minimization procedure of the cost function $J(x(t_0))$. One of the most important parts of the cost function is the background error covariance matrix B_0, of which the vertical component is determined by the vertical correlation model. The Gaussian correlation function is frequently used in various ionospheric data assimilation tools (Bust et al., 2004; Forsythe, Azeem, Blay, et al., 2021; Ssessanga et al., 2018). For example, in the Gaussian-Markov random field approximation of the precision matrix in NEDAM, the correlation lengths serve as scaling factors in the finite-difference matrix (Yuan et al., 2023).

In this section, we formalize the definition of the vertical correlation length VCL. Provided the error of electron density is regarded as a random variable of the altitude and the vertical correlation model is chosen to be a Gaussian correlation, the local VCL of the electron density errors can be calculated as follows:

$$\rho(x,y) = \frac{\mathrm{cov}(\epsilon_x,\epsilon_y)}{\sqrt{\mathrm{var}(\epsilon_x)\,\mathrm{var}(\epsilon_y)}} \quad (2)$$

$$\mathrm{VCL}(z) = \sqrt{-\Delta^2/\log(\rho(z,z+\Delta))} \quad (3)$$

where ϵ_x and ϵ_y represents the error of the ionosphere electron density model with respect to the ionosonde observations at heights x and y, respectively. $\mathrm{cov}(\epsilon_x,\epsilon_y)$ is the covariance between ϵ_x and ϵ_y, $\mathrm{var}(\epsilon_x)$ is the variance of the ϵ_x and Δ is the vertical step size, which is 5 km in this study. The validity of the choice of the Gaussian correlation function will be further discussed in Section 4.2. The VCL directly determines the vertical correlations via the Gaussian correlation function.

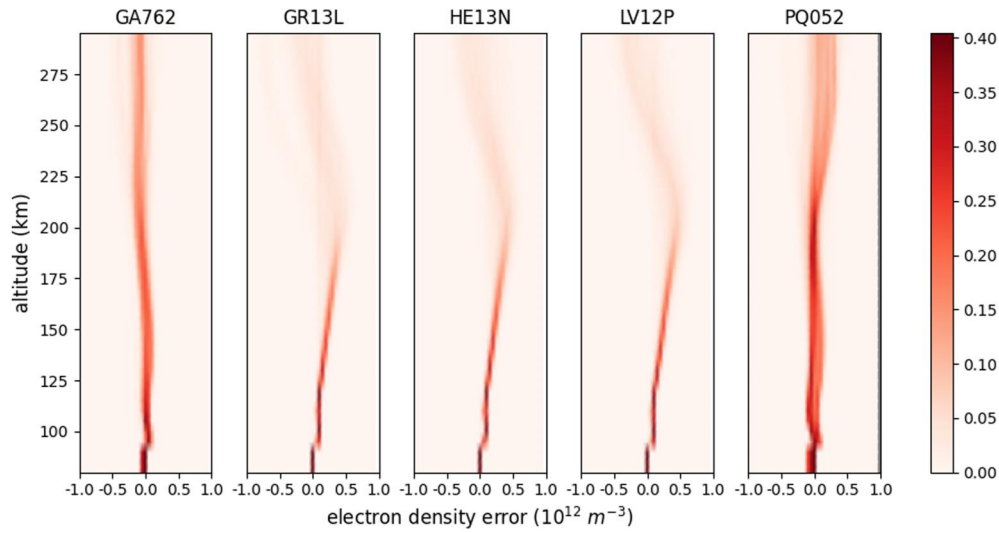

Figure 2. Probability distribution of the electron density error as a function of altitude for five ionosondes: GA762 (62.38°N, 145.0°W), GR13L (33.3°S, 26.5°E), HE13N (34.4°S, 19.2°E), LV12P (28.5° S, 21.2°E) and PQ052 (50.00°N, 14.6°E), considering all available observations in 2013. The color bar represents the probability of the electron density error.

Figure 2 shows the typical probability distribution of the electron density error at different altitudes from 80 to 300 km. In Figure 2, the probability distributions are very similar for the three closely located ionosondes, namely GR13L(33.3°S, 26.5°E), HE13N(34.4°S, 19.2°E) and LV12P(28.5°S, 21.2°E). And at all altitudes, there are evidently biases between the ionosphere model NEDM and ionosonde measurement, especially at altitudes below 200 km. For GA762 and PQ052 stations, the biases between the NEDM and ionosonde measurement are less pronounced than those for the three low-latitude stations. According to Schwarz inequality, the vertical correlation coefficient is a real number ranging from minus one to one. In practice, the error correlation coefficient is always non-negative within a finite range. And therefore, the VCL is well-defined by Equation 3. The choice of the electron density model influences the statistical analyses of ionospheric vertical correlations, since different models are developed based on different data and empirical parameterizations and formulations. In other words, the VCLs generated by one model may not be suitable for data assimilation with other models.

The locally defined VCLs are important for two main reasons. First, it is naturally assumed that two random variables at large spatial distances are independent. In practical applications, this assumption leads to a tapering of the covariance matrices, which means that the spatial correlation is non-zero within a finite distance. The second reason is that in the ionosphere, the electron density can vary by more than five orders of magnitude from the E region to the F region. If the variance masks used in the data assimilation are proportional to the background values, the large difference in magnitude of the variance masks also implies zero correlations for any two random variables at large distances. Otherwise, the increments of the electron densities with smaller variances in each assimilation step will be completely controlled by the electron densities with larger variances. In general, a localization procedure is used in the construction of a sparse covariance matrix. For the two reasons above, there is a strong case for the use of locally defined VCLs.

3.2. Statistical Characterization of VCLs

In ionospheric data assimilations, we are interested in the weather instead of the climatology. Simply speaking, the ionospheric weather is subject to variations of many physical states that are not considered in the climatological model. This fact implies that the climatological model can be assumed to be uncorrelated with the measurements when modeling the VCLs. Suppose that the electron density from the model and measurements can be regarded as two random variables X and X_1 with the parameter being altitude z and the climatological model is uncorrelated with the measurements. Then, the vertical error covariance between the model and measurement can be estimated as follows

$$Y(z) = X(z) - X_1(z) \tag{4}$$

$$\sigma_Y^2(z) = \sigma^2(z) + \sigma_1^2(z) \tag{5}$$

where σ represents the square root of the corresponding variances. Consider the two random variables namely, Y at z and $z + \Delta$; the covariance between these two random variables can be written as

$$\begin{aligned}\mathrm{cov}(Y(z), Y(z+\Delta)) &= \mathrm{cov}(X(z) - X_1(z), X(z+\Delta) - X_1(z+\Delta)) \\ &= \mathrm{cov}(X(z), X(z+\Delta)) + \mathrm{cov}(X_1(z), X_1(z+\Delta))\end{aligned} \tag{6}$$

The corresponding correlation coefficient is

$$\rho(Y(z), Y(z+\Delta)) = \frac{\mathrm{cov}(Y(z), Y(z+\Delta))}{\sqrt{\sigma_Y^2(z)\sigma_Y^2(z+\Delta)}} \tag{7}$$

Assuming the model and measurement are correlated with themselves at different heights by a Gaussian correlation with VCL L and L_1, respectively.

$$\begin{aligned}\rho(X(z), X(z+\Delta)) &= \exp\left(\frac{-\Delta^2}{L^2(z)}\right) \\ \rho(X_1(z), X_1(z+\Delta)) &= \exp\left(\frac{-\Delta^2}{L_1^2(z)}\right)\end{aligned} \tag{8}$$

We get the general formula for the error correlation coefficient

$$\rho(Y(z), Y(z+\Delta)) = \frac{\sigma(z)\sigma(z+\Delta)\exp\left(\frac{-\Delta^2}{L^2(z)}\right) + \sigma_1(z)\sigma_1(z+\Delta)\exp\left(\frac{-\Delta^2}{L_1^2(z)}\right)}{\sqrt{\sigma_Y^2(z)\sigma_Y^2(z+\Delta)}} \tag{9}$$

Considering the simplest case in which the variances for both models and measurements are the same constant along the z direction, the correlation can be expressed by defining an effective VCL L_Y

$$\rho(Y(z), Y(z+\Delta)) = \exp\left(\frac{-\Delta^2}{L_Y^2(z)}\right) \tag{10}$$

$$L_Y^2(z) = \lim_{\Delta \to 0} \frac{-\Delta^2}{log\left(\frac{1}{2}\left(\exp\left(-\Delta^2/L^2(z)\right) + \exp\left(-\Delta^2/L_1^2(z)\right)\right)\right)} \tag{11}$$

In small Δ cases, the effective VCL can be expressed by the Taylor expansion

$$L_Y^2(z \pm \Delta) = \frac{2L^2(z)L_1^2(z)}{L^2(z) + L_1^2(z)} + \frac{\Delta^2\left(L^2(z) - L_1^2(z)\right)^2}{2\left(L^2(z) + L_1^2(z)\right)^2} + \mathrm{O}\left(\Delta^4\right) \tag{12}$$

If the ionosphere model and the corresponding measurements have identical VCLs, the error VCLs between them will indeed coincide. However, if the ionosphere model and the measurements have different VCLs, the effective VCLs will exhibit nonconstancy, primarily due to the non-zero nature of the second order term, unless $\Delta = 0$. In this case, the VCL is not a standard Gaussian correlation outside a small neighborhood of height z. This explains why the correlation coefficients at 180 km in Figure 5 diverge from the locally derived Gaussian distribution and why the green lines are slightly "wider" than the orange lines. We notice that $L_Y^2(z \pm \Delta)$ is an even function of Δ, which means that under ideal conditions, the rate of divergence exhibits symmetry in the vicinity of the height parameter z.

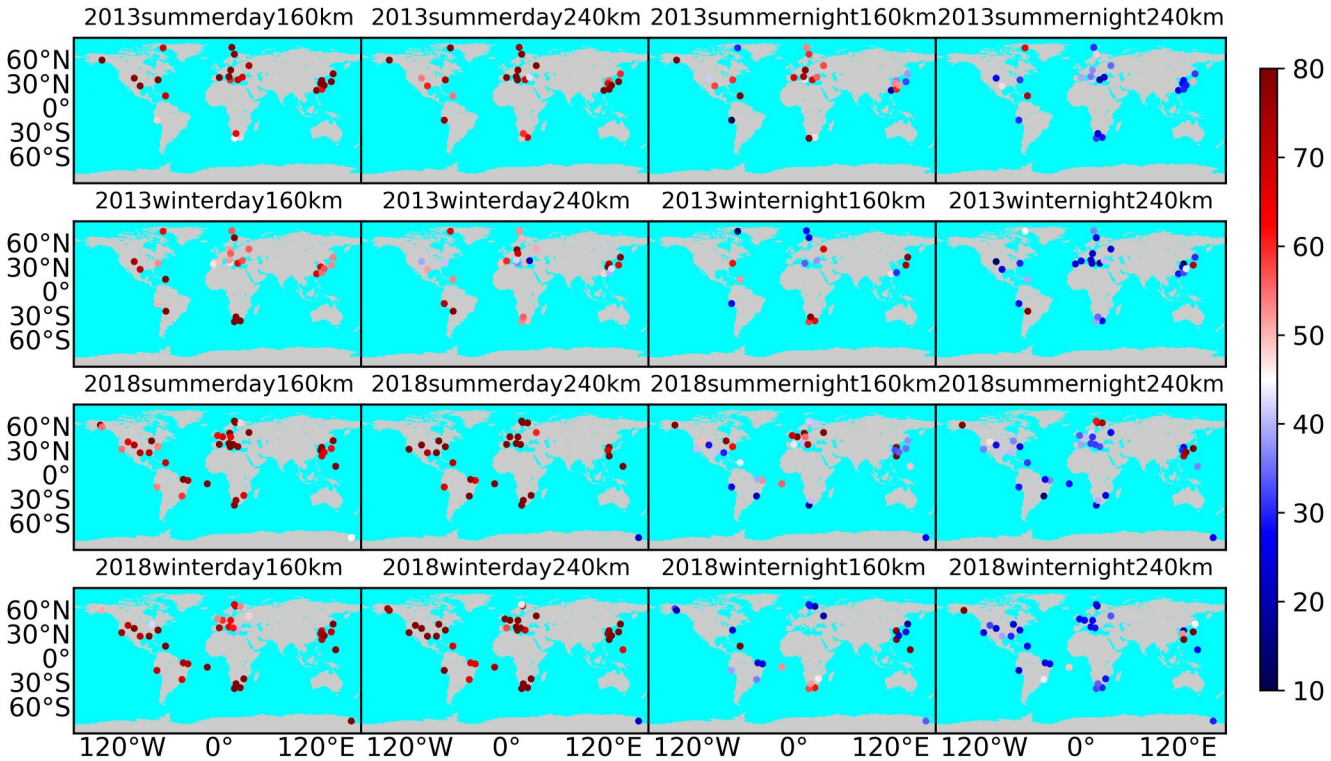

Figure 3. Global color-coded scatter plots of ionospheric VCLs. Unit: kilometers. Plots are binned into four different groups, that is, year (2013, 2018), season (summer, winter), local time (day, night) and altitude (160 km, 240 km).

If the variance ratio $k(z) = \sigma(z)/\sigma_1(z)$ is not identical to 1, the effective VCL in Equation 11 and the Taylor expansion in Equation 12 become

$$L_Y^2(z) = \lim_{\Delta \to 0} \frac{-\Delta^2}{log\left(\frac{k^2(z)\exp\left(-\Delta^2/L^2(z)\right)+\exp\left(-\Delta^2/L_1^2(z)\right)}{k^2(z)+1}\right)}$$

$$L_Y^2(z \pm \Delta) = \frac{\left(k^2(z)+1\right)L^2(z)L_1^2(z)}{L^2(z)+k^2(z)L_1^2(z)} + \frac{k^2(z)\Delta^2\left(L^2(z)-L_1^2(z)\right)^2}{2\left(L^2(z)+k^2(z)L_1^2(z)\right)^2} + \mathrm{O}\left(\Delta^4\right) \quad (13)$$

We note that in commonly used ensemble or Monte Carlo methods, the "virtual" observations are sometimes taken to be the average of the ensembles. In this case, the simulated VCL converges to the climatological VCL which is defined and estimated in the Appendix A. As is described in the Appendix A, the climatological VCL can be expressed as

$$L_{\mathrm{clim}} = \frac{2H^2}{\tau\alpha} \quad (14)$$

where H is the local scale height, τ is the standard deviation of the perturbation of the model driver, α is the slope of the scale height with respect to the model driver. Equation 14 illustrates that the climatological VCL is not uniquely determined by the inherent characteristics of the ionospheric model in isolation. Instead, the climatological correlation is inextricably linked to the nature of the perturbations employed. Climatological VCLs typically exhibit values considerably larger than the local scale height of the ionospheric model. For example, if $\tau\alpha = 0.2H$, $L_{\mathrm{clim}} = 10H$.

It is important to emphasize that while ensemble methods are valuable for propagating error covariances in dynamical systems over time, their applicability may be less suitable for generating vertical correlations in the

10.1029/2023SW003743

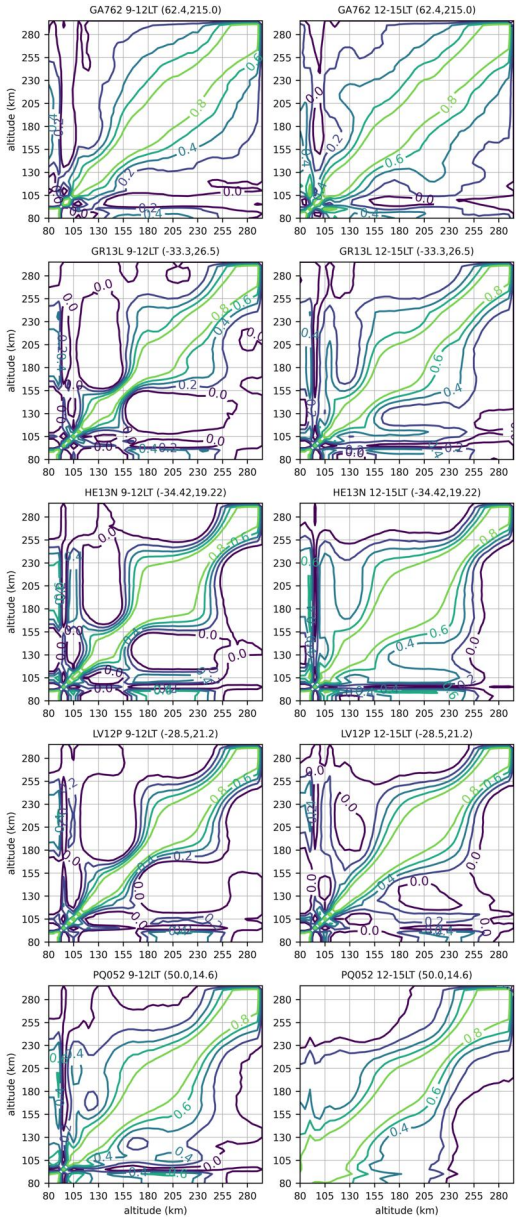

Figure 4. Pearson correlation coefficients for five different ionosondes: GA762, GR13L, HE13N, LV12P, and PQ052. The first column shows the correlation coefficients during 9–12 hr LT and the second column shows the correlation coefficients during 12–15 hr LT. The numbers in brackets are the geographical latitude and longitude of the ionosonde stations.

context described in this work. This assertion is consistent with previous ensemble experiments with empirical models, such as the IRI2016 with Chapman-fitted incoherent scatter radar observations and NeQuick-Az with ensemble methods (Aa et al., 2022; Forsythe, Azeem, Crowley, & Themens, 2021).

4. Results and Discussion

4.1. Local Time and Seasonal Variation

Figure 3 shows the ionospheric VCLs and demonstrates the possible dependencies of VCLs on local time and geographical seasons. It is intuitive to believe that the VCL should vary with local times, since the ionosphere photo-chemical reactions play an essential role in the vertical correlations. The behaviors of ionospheric vertical error correlations differ significantly during local daytime and nighttime. By comparing the first two columns and last two columns, it is evident that at both 160 and 240 km, the VCLs show the day-night asymmetry.

In Figure 3, there is a clear distinction between daytime and nighttime VCLs, indicating a pronounced diurnal variation and suggesting weaker vertical correlations during nighttime hours. The underlying rationale for this temporal disparity can be attributed to the ionospheric structural organization governed by Chapman theory during daylight hours. In cases where the photoionization process dominates electron production, higher correlation coefficients, or equivalently larger VCLs, are expected between electron densities at different heights due to the deterministic influence of solar radiation on electron density variations. Comparing daytime VCLs during the northern summer and winter seasons, there is no significant difference between the two seasons, which agrees with the previous studies (Forsythe, Azeem, Crowley, & Themens, 2021).

However, during nighttime intervals, the negligible influence of solar radiation on the photoionization process leads to a scenario where the nighttime electron density behavior at different altitudes may be subject to different mechanisms. These mechanisms, which include local ionospheric electrodynamics, atmospheric waves, and particle precipitation, suggest that nighttime electron densities may not exhibit as robust vertical correlations as their daytime counterparts. Furthermore, there is an observable non-uniformity in VCL distributions across latitudes. The complexity of nighttime VCLs suggests separate considerations of daytime and nighttime VCL modeling.

4.2. Gaussian Nature of Ionospheric Vertical Error Correlations

Figure 4 shows the five examples of vertical error correlation coefficients derived from ionosonde obervations at different latitudes. These five ionosondes are selected according to latitudes, that is, low latitude (GR13L, HE13N and LV12P), mid latitude (PQ052) and high latitude (GA762). We can see that at around 150 km the high correlation area for GA762 and 9–12hr LT is narrowing, which implies equivalently a decrease in VCL. The narrowing effect is greater in low and mid latitudes. However, the overall correleation distributions for three low latitude ionosondes are different from that for mid and high latitude ionosondes. The change in contours of the correlation coefficient away from the diagonal is rapid in the forenoon low latitude stations, which is shown by larger areas inside the zero (purple) contour lines. In the lower ionosphere below 120 km, the vertical correlations seem to have no well-organized structure. The VCL in the lower ionosphere is significantly smaller than that in the F layer.

10.1029/2023SW003743

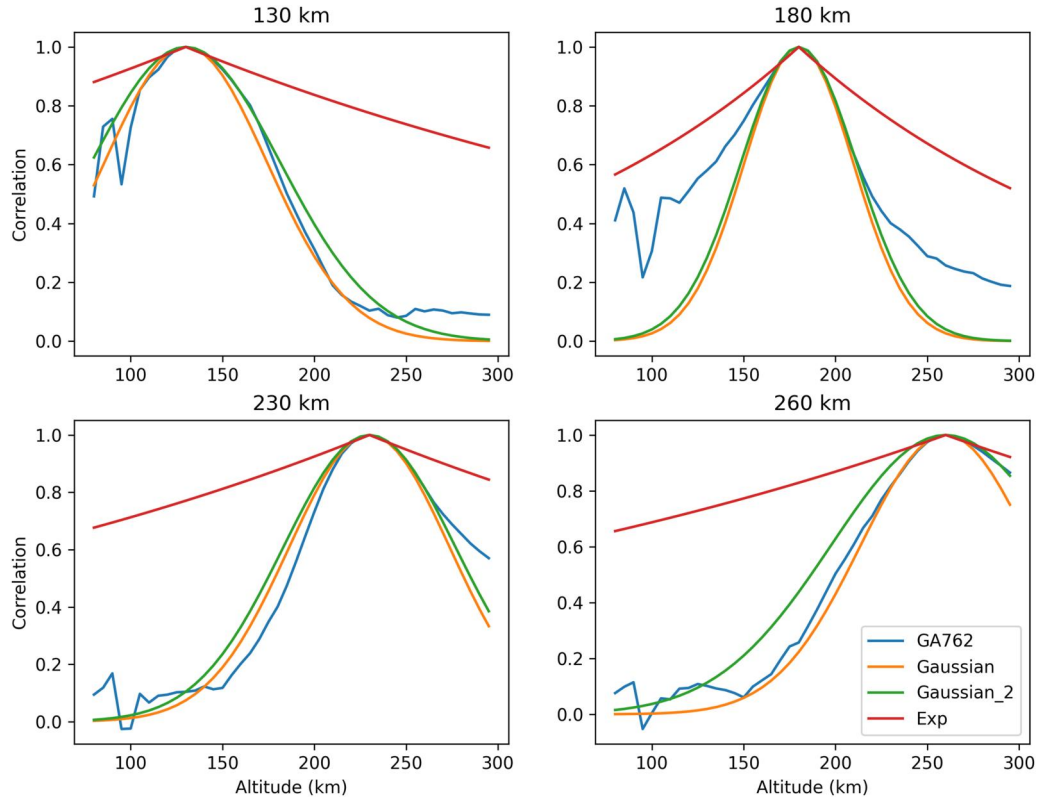

Figure 5. Three different correlation modeling cases, that is, the truth calculated from Equation 1, Gaussian model based on the VCL from Equation 2, Gaussian2 model based on the VCL from Equation 2 but by using the second nearby point, and exponential correlation case based on VCL, locally estimated by exponential correlation functions for the ionosonde station GA762 and different reference altitudes from 130 to 260 km during 9–15 hr LT in 2013.

By comparing the two columns in Figure 4, it can be seen that the vertical correlations have similar structures during 9–12hr LT and 12–15hr LT. But the correlations during 12–15hr LT are slightly larger than those during 9–12hr LT at the same altitudes for all five ionosondes. The zero contour lines expand outwards significantly for those three low latitude ionosondes. From the correlation patterns shown in Figure 4, it is evident that the correlation coefficients decrease rapidly along with changes of altitudes in the vicinity of the diagonals, which, to some extent, supports the idea of local definition of the VCL.

In previous studies on ionospheric data assimilations, the Gaussian correlation functions are commonly used. But the VCL in the Gaussian function may not be uniquely defined. For example, the VCL may be defined as the distance at which the correlation is equal to 0.7. The disadvantage of this definition is the potential break of local symmetry of the covariance matrix. On the other hand, this definition ignores the local behavior and focus on the spatially "average" behavior within a certain distance. However, we are more interested in the local behavior of error correlations than the far-field behavior, since the correlations decrease much faster in the far field. Provided the VCL is defined locally, it is essential to check if the locally derived correlation model can represent the true correlations in a larger distance or not. Figure 5 shows the examples of comparisons among three different correlation modeling cases, that is, the truth calculated from Equation 1, Gaussian model based on the VCL from Equation 2, Gaussian2 model based on the VCL from Equation 2 but by using the second nearby point, and exponential correlation case based on VCL locally estimated by exponential correlation functions. It is shown that the exponential correlation model is not able to describe the true correlation. In contrast, the two locally defined Gaussian correlation models, that is, the orange and green lines, fit the truth very well not only around the reference point but also in the region far away from the reference point, except the top right panel. For the reference point located at 180 km, the truth diverges from the locally defined Gaussian model outside the neighborhood of the reference point, which is also shown in Section 3.2.

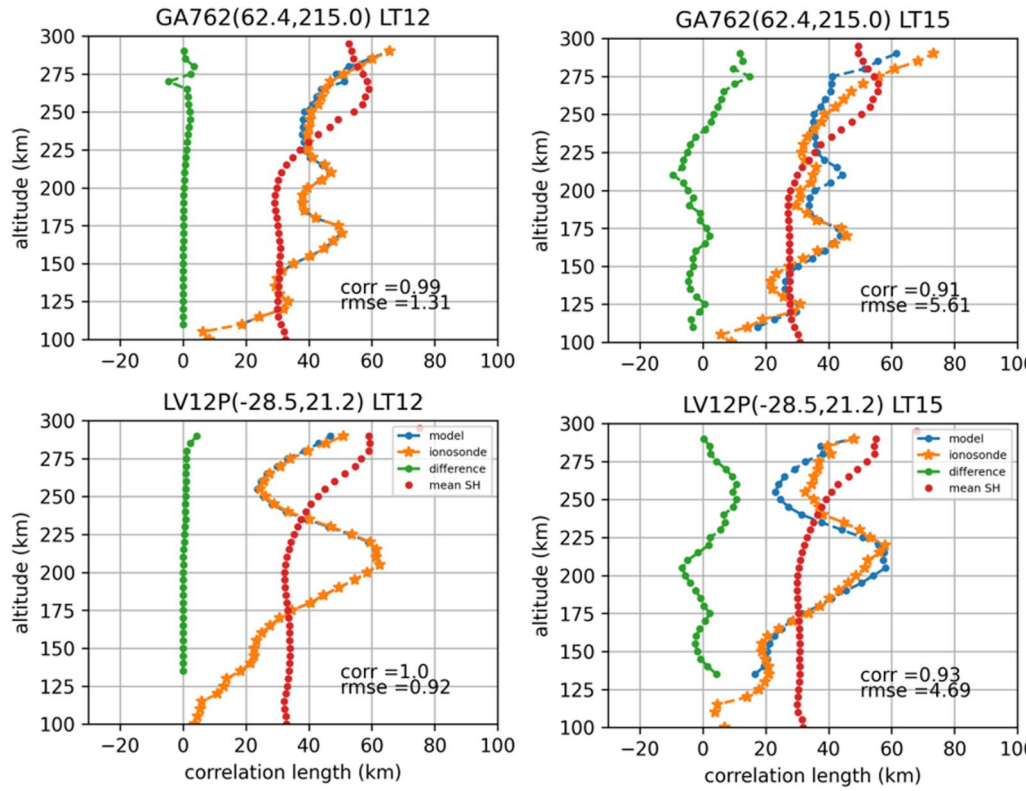

Figure 6. Validations of the vertical profiles of the error VCLs at two ionosonde stations, LV12P and GA762. The first column shows the modeling part and the second column shows the validation part. Blue (orange) lines represent the VCLs based on the optimized ratios (calculated from ionosonde observations). Green lines display the difference between the blue and orange lines. Red lines are the mean scale height (SH) based on ionosonde observations during each tested period.

4.3. Modeling the VCL: Two Case Studies

The ionospheric scale height can be a reasonable alternative for the VCL (Bust et al., 2004). It holds considerable promise if the VCLs can be effectively modeled in terms of the corresponding ionospheric scale heights. Implementing a correlation model where the variable is represented by scale heights proves practical, since empirical and physics-based ionospheric models typically provide scale height.

The vertical scale height in the Chapman theory can be derived from the electron density profile (Hernández-Pajares et al., 2017; Hoque et al., 2023). The vertical scale height can be estimated using the following equation

$$\mathrm{N}(\hat{h}) = N_m \exp\left((1/2) * \left(1 - \hat{h} - e^{-\hat{h}}\right)\right) \tag{15}$$

where $N(\hat{h})$ is the electron density at reduced height $\hat{h} = (h - hmF2)/H$, N_m is the maximum electron density of the F2 layer, and H is the vertical scale height.

To achieve an accurate representation of the VCLs, it is imperative to establish a fundamental relationship between the VCLs L and the associated scale height H. Ionosphere models exhibit stronger vertical correlations compared to ionospheric observations, for example, from ionosondes. According to Equation 14, we define the ratio of VCL to scale height as 5 for models and 0.5 for ionosonde observations. The remaining task is to find the vertical profile of the optimal variance ratio k based on ionosonde observations. However, the determination of this "optimal" ratio is a complex task, as there are different methodologies for its definition. For example, one approach could be to search for the optimal ratio that minimizes the standard deviation of each error VCL estimated from Equation 12. This method is inherently flawed because VCLs have nonlinear dependencies on all the parameters involved. A more robust and comprehensive approach to defining the optimal ratio is to utilize all available observations. In particular,

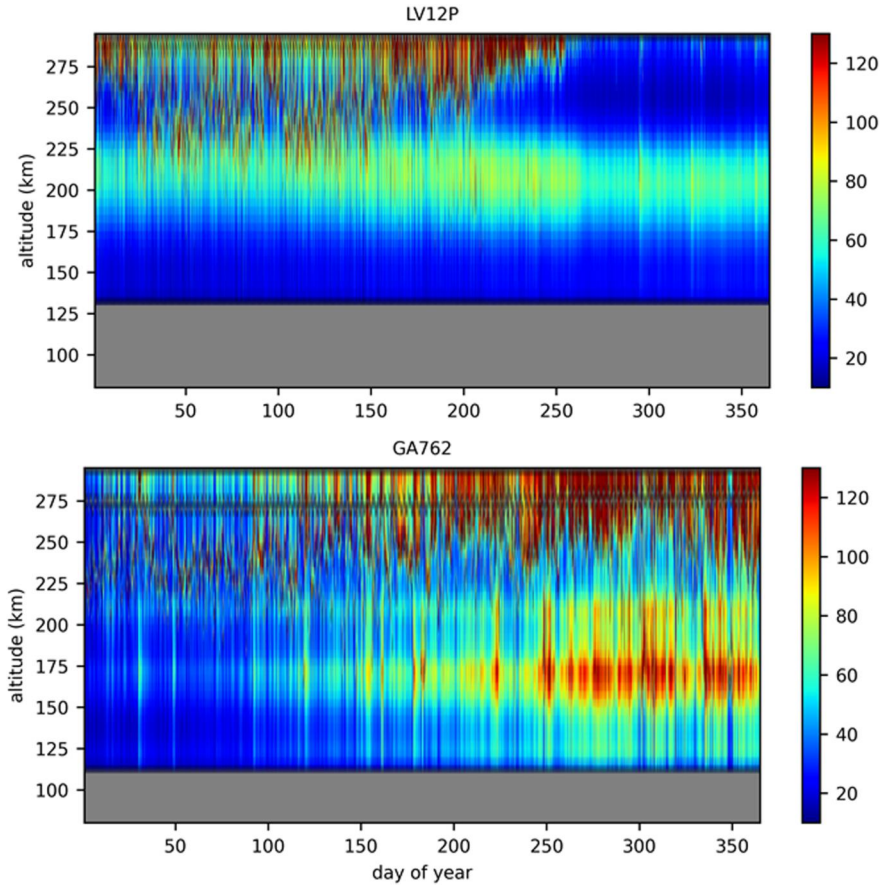

Figure 7. Color-coded temporal variations of modeled VCLs (unit: km) as a function of altitude for two ionosondes, LV12P and GA762, at 12 hr LT in 2013. The upper gray regions in both panels represent the hmF2 height in the NEDM ionospheric model.

by recognizing from Equation 12 that the reciprocal of the square of the VCL between two equally weighted independent random variables is equivalent to the mean of the reciprocals of the squares of the two original VCLs, a generalized approach can be easily formulated. Suppose during each observation window there are m different ionosphere states $\{X_1, X_2, \ldots, X_n\}$ observed by one ionosonde, then the errors $\{X\text{-}X_1, X\text{-}X_2, \ldots, X\text{-}X_n\}$ are equally weighted independent random variables. The VCL $\overline{L}$ that we calculate directly from Equation 3 will satisfy

$$\frac{n}{\overline{L}^2(z)} = \sum_{m=1}^{n} \frac{\left(k^2(z)+1\right)\hat{L}_m^2(z)L_m^2(z)}{\hat{L}_m^2(z)+k^2(z)L_m^2(z)} \tag{16}$$

$$\hat{L}_m^2(z) = 5\hat{H}_m(z)$$

$$L_m(z) = 0.5H_m(z) \tag{17}$$

where $\overline{L}(z)$ is the VCL calculated by Equation 3, $\hat{L}_m(z)$ is the mth VCL from the ionosphere model at altitude z, $L_m(z)$ is the mth ionosonde VCL at altitude z, $\hat{H}_m(z)$ is the mth ionospheric scale height from the ionosphere model at altitude z and $H_m(z)$ is the mth ionospheric scale height from the ionosonde observations. On the right hand side of Equation 16, there is only the unknown variance ratio $k(z)$ for each altitude z.

In this way, we could estimate the optimal ratio and two experiments are conducted for LV12P and GA762 ionosondes using observations throughout the year 2013. First we estimate the optimal ratio using the ionosonde observations from 12 to 13hr local time. The modeling results are shown in the first column of

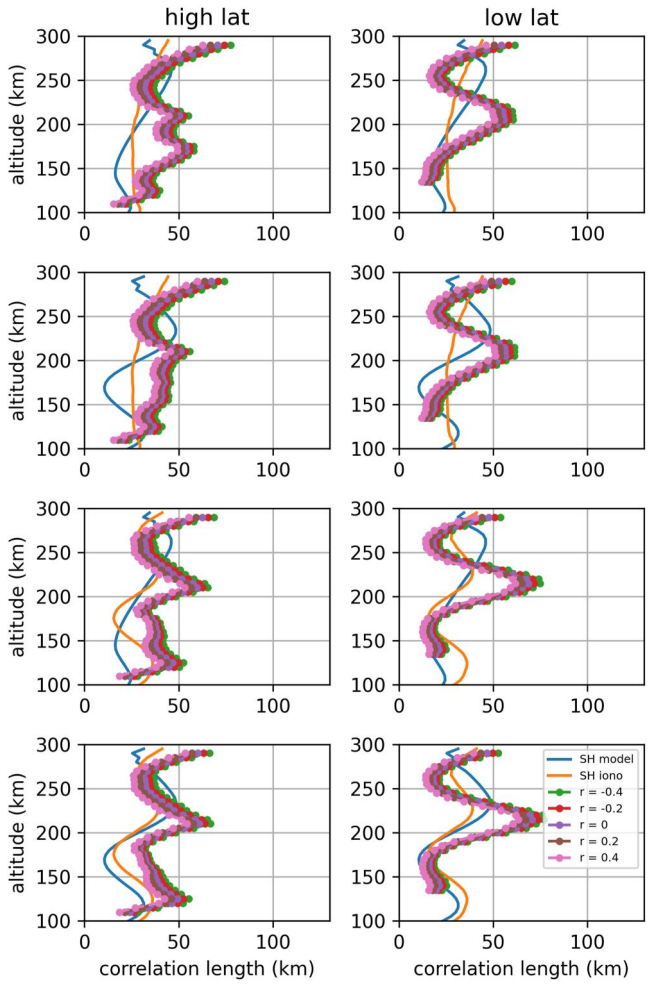

Figure 8. Modeled VCLs based on ionospheric climatological scale height (SH model; blue) and ionosonde scale height (SH iono; orange). The dotted lines in different colors represent modeled VCLs for different values of the correlation coefficient r between the ionosphere model and the observations.

Figure 6. The validation is conducted by the same procedure using the optimal ratio in the first step, but for another period which we choose to be 15–16hr local time here. The validation results are shown in the second column of Figure 6. In the lower E region below 130 km, correlation model values are missing simply because the Chapman layer assumption is not valid in this region and the proposed correlation model is not well-defined. This observation underscores that, below 130 km, the scale height may not be a suitable indicator for characterizing error VCLs. In practical applications, the model gap can be simply filled with the lowest value of the modeled VCLs.

Several notable observations concern the vertical correlation model. First, it is evident that the ratio between the model-derived VCLs and the scale height exhibits variations depending on the specific ionospheric model used. For this reason, a separate parameterization of the vertical correlation models for different ionospheric models will be necessary. Second, it is crucial to recognize that the ionospheric state is subject to daily variations. Therefore, the computed ionospheric correlation coefficients and lengths based on daily ionosonde observations may not fully adhere to statistical idealities, as it is not possible to reproduce the same ionospheric state in an infinite number of simultaneous measurements. Finally, it should be emphasized that the proposed methodology has a generic applicability that extends to other empirical ionospheric models that encapsulate ionospheric climatology.

Figure 7 shows a color-coded representation of the temporal dynamics of the modeled VCLs with respect to altitude for two ionosondes, LV12P and GA762, during 12hr LT in 2013. The upper gray regions in Figure 7 represent the hmF2 height in the NEDM ionospheric model. It is easy to see that the modeled VCLs show remarkable variations on different days of the year. In particular, for LV12P, the modeled VCLs show comparatively less variation compared to GA762. This discrepancy seems to be correlated with the scale heights obtained from ionosonde observations. In the upper F region above approximately 250 km, the temporal variations of VCLs are related with the extrapolations of the ionosonde-derived electron density profiles and therefore not physically true. Modeling VCLs in the upper ionosphere and plasmasphere may need the inclusion of radio occultation or incoherent scatter radar observations.

In the case of GA762 in Figure 7, the modeled VCLs show a distinct temporal pattern, increasing from about 30 km at the beginning of the year to more than 80 km in the second half of the year at the altitude of 170 km. Analogous increases in VCL values are observed at 210 km altitude. It is important to recognize that such dynamic changes in the modeled VCLs can have a noticeable influence on the results of data assimilation procedures, especially when multiple kinds of data with different geometries are included in the assimilation.

Figure 8 shows an example of modeled VCLs based on different types of ionospheric climatological scale heights and ionosonde-derived scale heights. The solid blue and orange lines correspond to the ionospheric climatological scale height and the ionosonde-derived scale height from actual ionosonde data, respectively. The dotted lines in different colors represent modeled VCLs for different correlation coefficient *r* values between the ionosphere model and the observations. The top row shows a typical set of scale heights, while subsequent rows show the same typical scale heights perturbed by a sinusoidal increment with a spatial period of 100 km and an amplitude of 10 km.

The proposed model is inherently dynamic, implying that as scale heights vary in time, either from observations or ionospheric models, the modeled VCLs adapt in accordance with these changes in scale heights. The results obtained from this representation show a consistent pattern: as the observed ionospheric scale height decreases, the corresponding VCLs show a concomitant decrease. This observation is consistent with the imperative need

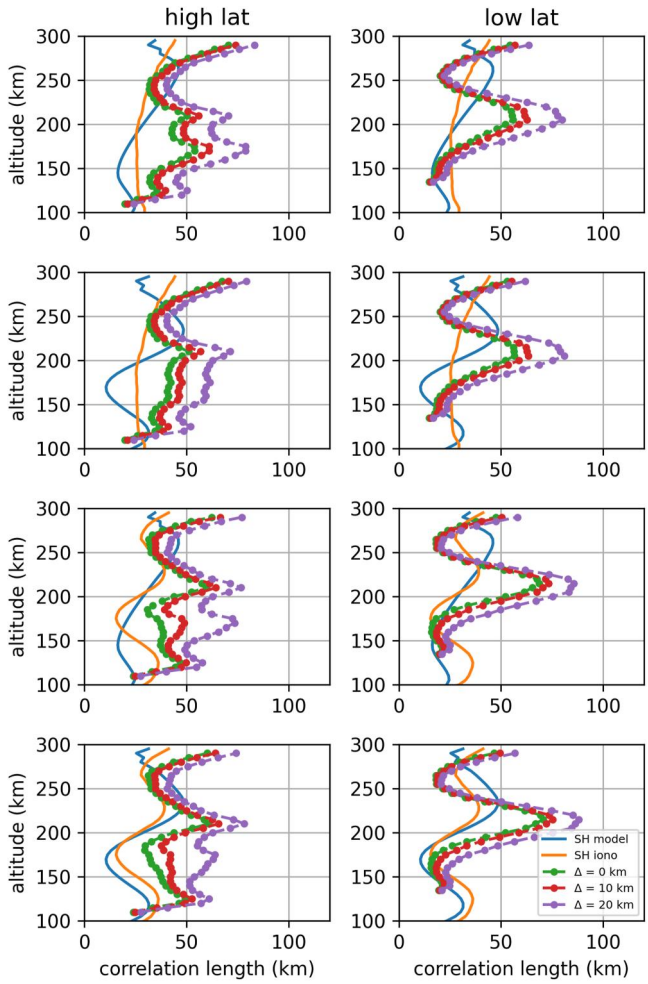

Figure 9. Modeled VCLs based on ionospheric climatological scale height (SH model; blue) and ionosonde scale height (SH iono; orange). The dotted lines in different colors represent modeled VCLs for different values of Δ.

to resolve finer ionospheric structures, especially when encountering larger vertical gradients. Figure 8 further illustrates the VCL profiles for different r values. Different r values represent different correlations between the ionosphere model and measurements. The presence of nonzero values of r is essential to ensure the existence of VCL values that extend beyond the boundaries of minimum and maximum scale heights, thereby accommodating a wider range of spatial correlations.

In this study, the higher order terms in Equation 13 are neglected when evaluating the VCL. Figure 9 shows the modeled VCLs for different values of Δ based on Equation 13, which includes the second order terms of Δ. As mentioned in Section 3.2, the VCLs will increase in the vicinity of the reference height when the climatological correlation lengths are different from the observed ionospheric correlation lengths, which is also shown in Figure 9. The inclusion of the second order terms has more complicated dependencies on the model and ionosonde scale heights than the zeroth order term shown in Figure 8. The inclusion of higher order terms provides chances to model the "flattened" correlation in the top right panel in Figure 5, which may be one of the main tasks for the VCL model parameter optimizations.

5. Conclusions

This study presents a comprehensive statistical analysis of the ionospheric vertical correlation length (VCL) using data from a global network of ionosondes. The main conclusions of this investigation are summarized as follows:

1. Locally derived VCLs were shown to have well-defined characteristics. In particular, the VCL shows limited dependence on solar flux or seasons, while exhibiting discernible local time dependencies. In general, daytime VCL values show a considerable increase compared to those observed at night, across all altitudinal regions.
2. For the first time, this study establishes that ionospheric VCLs can be effectively characterized by two primary parameters: the variance ratio and the correlation between the ionospheric model and the observational data, the latter being assumed to be zero in this study. VCL changes with altitude are mainly determined by a combination of inherent climatological and measured correlations. In addition, the study examines the relationships between climatological VCLs and scale heights within empirical ionospheric models.
3. Two experimental analyses were performed at the GA762 and LV12P ionosonde stations using the proposed model. The results show that the proposed model exhibits stability and a significant consistency with observed VCLs during daytime conditions, suggesting its potential for global correlation modeling.
4. The proposed models offer utility in the temporal evolution of error covariance matrices within ionospheric 4D-Variational assimilations, potentially mitigating one of the primary limitations associated with static error covariance specifications in such assimilation procedures.

Future research plans include the establishment of a global VCL model, achieved through parameter optimization using global electron density profiles over one or more solar cycles. In addition, the intricacies of nighttime correlations, which are more complex than their daytime counterparts and were not addressed in this study, could be the subject of further investigation. The proposed correlation model is intended for use in NEDAM as a scaling parameter in the Gaussian Markov Random Field approximation of the background precision matrices, as described in the work of Yuan et al. (2023). The performance of locally derived VCLs will be detailed in forthcoming research papers.

Appendix A: Derivation of the Climatological Vertical Correlation Length in Equation 14

From Equation 2, the vertical electron density gradient is

$$\frac{\partial N}{\partial h} = -\frac{N}{2H}\left(1 - e^{-\frac{h-hmF2}{H}}\right)$$

In the region that is far above the peak density height, which means that

$$\frac{h - hmF2}{H} \gg 1$$

we may drop the term $e^{-\hat{h}}$ in the gradient. Since $H(z)$ is a function of the model driver q, the perturbed scale height with a Gaussian perturbation $\Delta q \sim \mathcal{N}(0,\tau^2)$ is

$$H(q + \Delta q, z) = H(q,z) + \alpha(q,z)\Delta q + O\left((\Delta q)^2\right)$$

$$\alpha = \frac{\partial H}{\partial q}$$

The ionospheric electron density variations in the climatological model is composed by three parts which are the variation in NmF2, hmF2 and scale heights. For simplicity, we do not discuss the variation of NmF2 and hmF2 here. In the region that is far away from peak density height, the climatological correlations can be estimated as follows

$$r = z - hmF2$$

$$\Delta N(q + \Delta q, z) = \frac{r\alpha(q,z)\Delta q}{2H^2(q,z)} N(q,z)$$

$$\Delta N(q + \Delta q, z + \Delta) = N\left(1 - \frac{\Delta}{2H(q + \Delta q, z)}\right)\left(1 + \frac{r\alpha(q,z)\Delta q}{2H^2(q,z)}\right) - N\left(1 - \frac{\Delta}{2H(q,z)}\right)$$

$$\frac{\Delta}{2H(q + \Delta q, z)} = \frac{\Delta}{2H(q,z)}\left(1 - \frac{\alpha(q,z)\Delta q}{H(q,z)}\right)$$

$$\Delta N(q + \Delta q, z + \Delta) = \frac{\alpha(q,z)\Delta q(2\Delta H(q,z) + 2rH(q,z) + r\Delta)}{4H^3(q,z)} N(q,z) + \frac{r(\alpha(q,z)\Delta q)^2\Delta}{4H^4(q,z)} N(q,z)$$

The correlation coefficient becomes

$$\rho = \frac{\mathrm{cov}(\Delta N(q + \Delta q, z), \Delta N(q + \Delta q, z - \Delta z))}{\sqrt{\sigma_x^2 \sigma_y^2}}$$

$$\sigma_x^2 = \mathrm{cov}(\Delta N(q + \Delta q, z), \Delta N(q + \Delta q, z))$$

$$\sigma_y^2 = \mathrm{cov}(\Delta N(q + \Delta q, z + \Delta), \Delta N(q + \Delta q, z + \Delta))$$

Using the fact that for any random variable $X \sim \mathcal{N}(0,\sigma^2)$

$$\mathrm{var}(cX) = \mathrm{cov}(cX, cX) = c^2 \mathrm{var}(X) = c^2\sigma^2$$

$$\mathrm{cov}(X^2, X) = E(X^3) - E(X)\,E(X^2) = 0$$

$$\mathrm{var}(X^2) = 2\sigma^4$$

after substitution, the correlation coefficient γ becomes

$$\rho = \frac{1}{\sqrt{1 + \frac{2\alpha^2\Delta^2 r^2\tau^2}{H^2(2Hr + r\Delta + 2H\Delta)^2}}}$$

where all variables are evaluated at altitude z and Δ is small compared to the scale height H. The corresponding correlation length is

$$L(z+\Delta) = \frac{2H^2}{\tau\alpha} + \frac{(2H+r)}{Hr}\frac{H^2}{\tau\alpha}\Delta + \mathrm{O}(\Delta^2)$$

It is noted that the climatological correlations are asymmetrically distributed around altitude z due to the nontrivial first order term of Δ, which is different from Equation 13. The climatological VCL L_{clim} can be estimated by

$$L_{\mathrm{clim}} = \frac{2H^2}{\tau\alpha}(*)$$

In the region that is close to the peak density region, which means that

$$\beta = \left|\frac{h - hmF2}{H}\right| \ll 1$$

following the same procedure, the climatological VCL becomes

$$L_{\mathrm{clim}} = \frac{2H^2}{\tau\alpha\beta}$$

In the region that is far below hmF2 height, which means that

$$\frac{h - hmF2}{H} < -1$$

the climatological VCL is similar to the first case.

$$L_{\mathrm{clim}} \sim \frac{H^2}{\tau\alpha}$$

It is clear now that the uncorrelated part comes from the nonlinear term $(\Delta q)^2$. Following the same computation, it can be shown that NmF2 and hmF2 variations of the first order do not contribute to the uncorrelated part, which implies that in general the omission of NmF2 and hmF2 in the above discussion is reasonable.

Data Availability Statement

All available ionosonde data from GIRO data sets can be downloaded from https://www.ngdc.noaa.gov/stp/IONO/.

Acknowledgments
The authors thank the GIRO group for providing global ionosonde data. The authors also thank the Institute of Data Science of the German Aerospace Center for providing resources on the High Performance Cluster. The work was carried out within the programmatic funding of the German Aerospace Center. Open Access funding enabled and organized by Projekt DEAL.

References

Aa, E., Zhang, S.-R., Erickson, P. J., Wang, W., Coster, A. J., & Rideout, W. (2022). 3-D regional ionosphere imaging and SED reconstruction with a new TEC-based ionospheric data assimilation system (TIDAS). *Space Weather*, *20*(4), e2022SW003055. https://doi.org/10.1029/2022SW003055

Bust, G. S., & Crowley, G. (2007). Tracking of polar cap ionospheric patches using data assimilation. *Journal of Geophysical Research*, *112*(A5), A05307. https://doi.org/10.1029/2005JA011597

Bust, G. S., & Datta-Barua, S. (2014). *Scientific investigations using IDA4D and EMPIRE, (chap. 23)* (pp. 283–297). American Geophysical Union (AGU). https://doi.org/10.1002/9781118704417.ch23

Bust, G. S., Garner, T. W., & Gaussiran, T. L. (2004). Ionospheric data assimilation three-dimensional (IDA3D): A global, multisensor, electron density specification algorithm. *Journal of Geophysical Research*, *109*(A11), A11312. https://doi.org/10.1029/2003JA010234

Bust, G. S., & Mitchell, C. N. (2008). The history, current state, and future directions of ionospheric imaging. *Reviews of Geophysics*, *46*(1), RG1003. https://doi.org/10.1029/2006RG000212

Codrescu, S. M., Codrescu, M. V., & Fedrizzi, M. (2018). An ensemble Kalman Filter for the thermosphere-ionosphere. *Space Weather*, *16*(1), 57–68. https://doi.org/10.1002/2017SW001752

Daley, R. (1991). *Atmospheric data analysis, Cambridge atmospheric and space science series*. Cambridge University Press.

Forsythe, V. V., Azeem, I., Blay, R., Crowley, G., Gasperini, F., Hughes, J., et al. (2021). Evaluation of the new background covariance model for the ionospheric data assimilation. *Radio Science*, *56*(8), e2021RS007286. https://doi.org/10.1029/2021RS007286

Forsythe, V. V., Azeem, I., & Crowley, G. (2020). Ionospheric horizontal correlation distances: Estimation, analysis, and implications for ionospheric data assimilation. *Radio Science*, *55*(12), e2020RS007159. https://doi.org/10.1029/2020RS007159

Forsythe, V. V., Azeem, I., Crowley, G., & Themens, D. R. (2021). Ionospheric vertical correlation distances: Estimation from ISR data, analysis, and implications for ionospheric data assimilation. *Radio Science*, *56*(2), e2020RS007177. https://doi.org/10.1029/2020RS007177

Hernández-Pajares, M., Garcia-Fernàndez, M., Rius, A., Notarpietro, R., Engeln, A., Olivares-PulidoOlivares-Pulido, G. G., et al. (2017). Electron density extrapolation above F2 peak by the linear vary-chap model supporting new global navigation satellite systems-LEO occultation missions. *Journal of Geophysical Research: Space Physics*, *122*(8), 9003–9014. https://doi.org/10.1002/2017JA023876

Hoque, M. M., & Jakowski, N. (2011). A new global empirical NmF2 model for operational use in radio systems. In *Radio science* (Vol. 46, pp. 1–13). https://doi.org/10.1029/2011RS004807

Hoque, M. M., & Jakowski, N. (2012). A new global model for the ionospheric F2 peak height for radio wave propagation. *Annals of Geophysics*, *30*(5), 797–809. https://doi.org/10.5194/angeo-30-797-2012

Hoque, M. M., Jakowski, N., & Prol, F. S. (2022). A new climatological electron density model for supporting space weather services. *Journal of Space Weather and Space Climate*, *12*, 1. https://doi.org/10.1051/swsc/2021044

Hoque, M. M., Yuan, L., Prol, F. S., Hernández-Pajares, M., Notarpietro, R., Jakowski, N., et al. (2023). A new method of electron density retrieval from MetOp-A's truncated radio occultation measurements. *Remote Sensing*, *15*(5), 1424. https://doi.org/10.3390/rs15051424

Jakowski, N., & Hoque, M. M. (2018). A new electron density model of the plasmasphere for operational applications and services. *Journal of Space Weather and Space Climate*, *8*, A16. https://doi.org/10.1051/swsc/2018002

Jakowski, N., Hoque, M. M., & Mayer, C. (2011). A new global TEC model for estimating transionospheric radio wave propagation errors. *Journal of Geodynamics*, *85*(12), 965–974. https://doi.org/10.1007/s00190-011-0455-1

Kodikara, T., Zhang, K., Pedatella, N. M., & Borries, C. (2021). The impact of solar activity on forecasting the upper atmosphere via assimilation of electron density data. *Space Weather*, *19*(5), e2020SW002660. https://doi.org/10.1029/2020SW002660

Rishbeth, H., & Garriott, O. K. (1969). *Introduction to ionospheric physics*. Academic Press.

Scherliess, L., Schunk, R. W., Sojka, J. J., Thompson, D. C., & Zhu, L. (2006). Utah State University global assimilation of ionospheric measurements Gauss-Markov Kalman filter model of the ionosphere: Model description and validation. *Journal of Geophysical Research*, *111*(A11), A11315. https://doi.org/10.1029/2006JA011712

Shim, J. S., Scherliess, L., Schunk, R. W., & Thompson, D. C. (2008). Spatial correlations of day-to-day ionospheric total electron content variability obtained from ground-based GPS. *Journal of Geophysical Research*, *113*(A9), A09309. https://doi.org/10.1029/2007JA012635

Ssessanga, N., Kim, Y. H., Choi, B., & Chung, J.-K. (2018). The 4D-var estimation of North Korean rocket exhaust emissions into the ionosphere. *Journal of Geophysical Research: Space Physics*, *123*(3), 2315–2326. https://doi.org/10.1002/2017JA024596

Yuan, L., Hoque, M. M., & Kodikara, T. (2023). The four-dimensional variational neustrelitz electron density assimilation model: NEDAM. *Space Weather*, *21*(6), e2022SW003378. https://doi.org/10.1029/2022SW003378

Yue, X., Schreiner, W. S., Lin, Y.-C., Rocken, C., Kuo, Y.-H., & Zhao, B. (2011). Data assimilation retrieval of electron density profiles from radio occultation measurements. *Journal of Geophysical Research*, *116*(A3), A03317. https://doi.org/10.1029/2010JA015980

Yue, X., Wan, W., Liu, L., & Mao, T. (2007). Statistical analysis on spatial correlation of ionospheric day-to-day variability by using GPS and incoherent scatter radar observations. *Annales Geophysicae*, *25*(8), 1815–1825. https://doi.org/10.5194/angeo-25-1815-2007

Yue, X., Wan, W., Liu, L., Zheng, F., Lei, J., Zhao, B., et al. (2007). Data assimilation of incoherent scatter radar observation into a one-dimensional midlatitude ionospheric model by applying ensemble Kalman filter. *Radio Science*, *42*(6), RS6006. https://doi.org/10.1029/2007RS003631